Toroidal Plasma Current Startup and Sustainment by rf in the WT-2 Tokamak

S. Kubo, M. Nakamura, T. Cho, S. Nakao, T. Shimozuma, A. Ando,
K. Ogura, T. Maekawa, Y. Terumichi, and S. Tanaka
Department of Physics, Faculty of Science, Kyoto University, Kyoto 606, Japan

(Received 14 March 1983)

By injecting the lower hybrid wave into the microwave discharge plasma at the electron-cyclotron resonance in the WT-2 toroidal device, the toroidal plasma current is generated, started up to $I_p \simeq 5$ kA, and sustained by rf power alone, without the Ohmic heating power (rf tokamak). This lower-hybrid-wave–driven current is produced only when high-energy tail electrons, which interact resonantly with the lower hybrid wave, are present in the initial electron-cyclotron resonance plasma.

PACS numbers: 52.50.Gj, 52.55.Gb

Recently rf current drive has received much interest since generating and sustaining a continuous toroidal current comprise one of the most important problems to be settled in order to realize steady operation of a tokamak reactor. Theories have predicted that a fast electron beam carrying the current is produced by quasilinear Landau damping of lower hybrid waves (LHW).[1-3] Experiments showed that the LHW-driven current was produced in the Ohmically heated (OH) plasmas[4-7] and further that the Ohmic current is replaced completely by the LHW-driven current by injecting LHW at the end of a tokamak discharge.[8-10] In this Letter, we report the first experiment in the WT-2 toroidal device for which the toroidal plasma current is started up and sustained by rf only, without the Ohmic heating power. Here, an initial plasma is produced by a microwave discharge at the electron-cyclotron resonance (ECR plasma) and the LHW is injected.

The WT-2 tokamak[5,8] has an aluminum shell, major and minor radii $R = 40$ and $a = 9$ cm, respectively, and a toroidal field $B_T \lesssim 13$ kG. The ECR plasma is produced by injecting microwave power ($f = 35.6$ GHz, $P_{ECH} \lesssim 30$ kW, $T \lesssim 10$ ms) from a gyrotron into the topside of the vacuum vessel. In order to achieve the LHW current drive, rf power ($f = 915$ MHz, $P_{LHH} \lesssim 100$ kW, $T \lesssim 21$ ms) from a magnetron is launched into the plasma with a phased array of four waveguides (inner dimension 13×185 mm^2) with a phase difference of $\pi/2$ from each other. It is noted that no Ohmic power is applied and the primary winding of the Ohmic heating transformer is shorted.

When P_{ECH} is injected, the ECR plasma, with an electron density $\bar{n}_e \simeq 2 \times 10^{12}$ cm^{-3}, is produced and there appears a weak toroidal plasma current, $I_p \sim 0.5$ kA [Figs. 1(a) and 1(b)]. Next, when P_{LHH} is applied before termination of P_{ECH}, the current I_p starts up rapidly and attains $I_p \approx 5$ kA at the end of P_{LHH}, while $\bar{n}_e$ is kept constant. The loop voltage V_L is low ($V_L \approx -1$ V) and proportional to dI_p/dt. The direction of the electric field is such that it opposes the electron drift. Therefore, it is considered that the current I_p is started up and the LHW-driven current-sustained (LH-CS) plasma is produced in the initial ECR plasma by injecting rf power (P_{ECH} and P_{LHH}) only. Soft x-ray emission I_{sx} (0.85 keV) measured by a single-sideband detector[8] appears in the ECR plasma, and becomes very intense in the LH-CS plasma [Fig. 1(d)]. It is noted that the intensity is scaled down by $\frac{1}{25}$ for the latter plasma (bursts of I_{sx} will be described later). There is no hard x-ray emission from the ECR plasma, but hard x rays (40 keV) appear and become very strong when P_{LHH} is applied. Correspondingly, the electron-cyclotron second-harmonic emission I_μ (68 GHz), which is above the thermal radiation level in the ECR plasma, becomes intense in the LH-CS plasma. These strong emissions I_{sx}, I_{hx}, and I_μ suggest that nonthermal electrons are produced in the ECR plasma and the high-energy electron beam carrying the current I_p is generated by LHW.

Measurements by a Langmuir probe show an electron temperature $T_e \simeq 20$ eV for the ECR plasma. For the LH-CS plasma the probe measurement cannot be made, since the current I_p is interrupted by the probe. However, its temperature is estimated to be at the same order as that of the ECR plasma by comparison of the intensities of impurity lines (O II–O V) from both plasmas. In addition, the high-energy tail of electrons is present in both ECR and LH-CS plasmas. From the absorption method for I_{sx} the energy of the fast electrons is estimated to be 0.5–1 keV for the ECR plasma; 10–40 keV

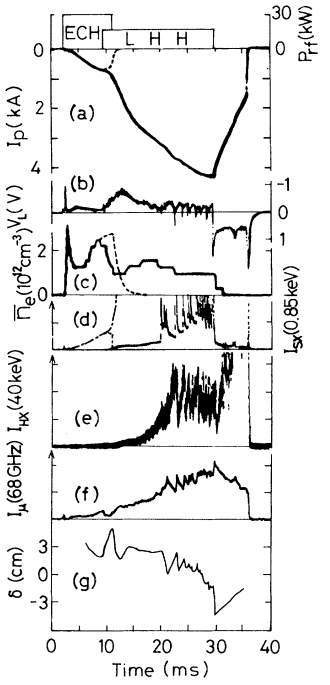

FIG. 1. Temporal evolution of (a) plasma current I_p, (b) loop voltage V_L, (c) vertically line-averaged electron density $\bar{n}_e$ measured by 4-mm interferometer, (d) soft x-ray emission I_{sx}, (e) hard x-ray emission I_{hx}, (f) cyclotron emission I_μ, and (g) plasma position signal δ. Full curves are for LH-CS plasma in ECR plasma and dotted ones for ECR plasma. $p = 6 \times 10^{-5}$ Torr in H_2 and the additional gas is puffing during the injection of P_{LHH}. $B_T = 13$ kG and $B_{v0} = 33$ G.

at $t \simeq 13$ ms and 30–50 keV at $t \simeq 20$ ms for the LH-CS plasma. The pulse-height analysis of I_{hx} shows that the maximum energy shifts from 40 to 300 keV during LHW injection. Thus, the electrons of the LH-CS plasma are composed of bulk electrons with $T_e \simeq 20$ eV, $n_e \simeq 1 \times 10^{12}$ cm^{-3} and fast beam electrons with energy $w_b \simeq 40$ keV, $n_b \simeq 1 \times 10^{10}$ cm^{-3}, which are carrying the current $I_p \approx 5$ kA.

In Fig. 1(b), during the later period of the LH-CS plasma, with $I_p \simeq 4$–5 kA ($t = 20$–30 ms), there appear sharp positive voltage spikes. Bursts of I_{sx} and I_{hx}, steplike increase of I_μ, and an abrupt inward displacement of the plasma δ are correlated with the voltage spikes [Figs. 1(d)–1(g)]. These characteristics are the same as those of the relaxation oscillations observed in the LH-CS plasmas produced during or after the OH plasma and ascribed to the anisotropic velocity distribution of electrons produced by LHW.[5,8] Thus, it is reasonable to consider that the LH-CS plasma produced in the ECR plasma

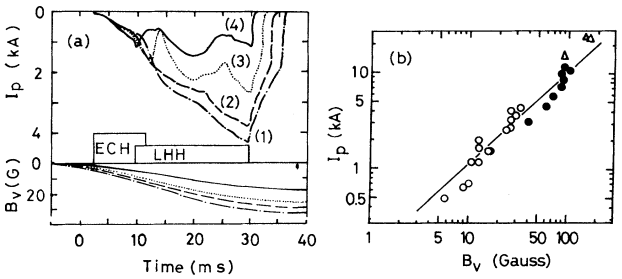

FIG. 2. (a) Temporal evolution of plasma current I_p for various values of vertical field B_v. (1) $B_{v0} = 33$, (2) 29, (3) 27, and (4) 18 G. $P_{ECH} = 30$ kW, $P_{LHH} = 20$ kW, $p = 6 \times 10^{-5}$ Torr. (b) Maximum values of I_p as a function of B_v. Data (open circles) obtained from the LH-CS plasmas produced in ECR plasma, (filled circles) LH-CS plasmas after Ohmically heated plasma, and (open triangles) from the Ohmically heated plasmas. The line shows the relation of magnetohydrodynamic equilibrium between I_p and B_v.

is the same as that produced after the OH plasma. After the P_{LHH} is turned off, the plasma is maintained for several milliseconds by consuming the stored magnetic energy ($L_p I_p^2/2 \simeq 15$ J). Here the intensity of I_{hx} increases strongly and I_μ is still intense, though I_p, n_e, and I_{sx} decrease. The result is explained by the fast electrons which are accelerated by the positive loop voltage, $V_L \approx 1$ V, in this period.

The vertical field B_v plays a quite important role for the current startup and sustainment. In Fig. 2(a), the maximum plasma current $I_{p\,max}$ is obtained at the end of the P_{LHH} for $B_{v0} \simeq 33$ G [curve (1)]. $I_{p\,max}$ decreases regardless of whether B_{v0} is increased or decreased. When $B_{v0} \simeq 27$ G, I_p suddenly decreases at $t \simeq 13$ ms and then increases again. Measurements of the temporal variation of the horizontal profile of I_{sx} (0.2 keV) with an array of six single-sideband detectors show that the plasma column is displaced outward and contacts the limiter when I_p decreases, then moves inward gradually as I_p increases again. When B_v is adjusted, the plasma column is near the center of the vessel and I_p attains a maximum value. Such maximum values of I_p are plotted as a function of B_v in Fig. 2(b). The solid line represents the relation of magnetohydrodynamic equilibrium for the tokamak current given by[11]

$$B_v = (\mu_0 I_p/4\pi R)\{\ln(8R/a) + \beta_p - \tfrac{3}{2} + l_i/2\},$$

where $R = 40$ and $a = 8$ cm, and $\beta_p = 1$ and $l_i = 1$ are assumed. The experimental plots agree well with the theoretical prediction. Thus, it is con-

cluded that the LH-CS plasma produced in the ECR plasma is in magnetohydrodynamic equilibrium. The safety factor at the plasma surface is estimated to be $q_a \simeq 17$ for $I_p \simeq 5$ kA. In Fig. 1(g), the center of the plasma current I_p is at $\delta \gtrsim 2$ cm in the ECR plasma. When P_{LHH} is applied, the position δ shifts outward quickly then moves toward the center and varies rapidly during the relaxation oscillation. Such movement of the plasma column is ascertained by the horizontal profile of I_{sx} (0.2 keV).

The plasma current I_p can be started up when P_{LHH} is injected into the ECR plasma produced in a low filling-gas pressure only ($p \lesssim 1\times10^{-4}$ Torr). In Fig. 3(a), the electron density $\bar{n}_e$ for the ECR plasma increases, while the temperature T_e decreases as the pressure p increases. The strong emission I_{sx} and current I_p are observed in the ECR plasma produced in the low-p region, suggesting that there are suprathermal electrons. When P_{LHH} is applied into these ECR plasmas both I_p and I_{sx} are enhanced drastically [Fig. 3(b)]. On the other hand, there appear weak I_{sx} and I_p in the ECR plasma produced in high-p region ($p \gtrsim 2\times10^{-4}$ Torr); and no enhancements of I_p and I_{sx} are observed when P_{LHH} is injected. The boundary of p increases with P_{ECH}. This result means that the presence of suprathermal electrons in the initial ECR plasma is necessary in order to start up I_p by injecting P_{LHH}. This is reasonable since only the suprathermal electrons can interact resonantly with LHW having the parallel refractive index $N_\parallel \lesssim 8$ (equivalent energy $\gtrsim 4$ keV). This fact may explain why the generation of the LHW-driven current is limited to low-density plasma[4-10] (density limit) in a slideaway regime of the tokamak discharge.

The computer simulation has been carried out in order to explain these physical processes. For electrons uniform in space, the Boltzmann equation contains the nonlinear Fokker-Planck collision term, the quasilinear diffusion terms of both electron-cyclotron waves (ECW) and LHW, and the energy-loss term; and the equation is solved numerically in the two-dimensional velocity space. The initial distribution of electrons is assumed to be Maxwellian with $T_e \simeq 50$ eV and $n_e = 1\times10^{12}$ cm^{-3}. The resonant region of ECW is $|v_\parallel/(10^9 \text{ cm/s})| < 4$, which is symmetric about $v_\parallel = 0$, while that of the LHW is $2 < v_\parallel/(10^9 \text{ cm/s}) < 8$. The quasilinear diffusion coefficients are assumed to be $D_{ECW} \simeq 0.05 D_{coll}$ and $D_{LHW} \simeq 0.5 D_{coll}$, respectively, where $D_{coll} = 5\times10^{22}$ cm^2/s^3 is a usual collisional diffusion coefficient. The ions are maintained fixed Maxwellian with $T_i = 30$ eV. No plasma current density J_p appears during P_{ECH}. When P_{LHH} is turned on, the current J_p starts up and increases linearly in time and the velocity distribution function $f(v_\parallel, v_\perp)$ is changed as shown in Figs. 4(b)–4(d). While the electrons are accelerated only in the perpendicular direction by P_{ECH}, they are pitch-angle scattered to the parallel direction via e-e and e-i collisions. Such suprathermal electrons with $v_\parallel \gtrsim 2\times10^9$ cm/s can interact with LHW and are quasilinearly diffused into the high-$v_\parallel$ region, resulting in production of J_p. After P_{ECH} is turned off, the quasilinear plateau is formed and J_p is saturated. It is noted that no current is produced when P_{LHH} is applied to the initial

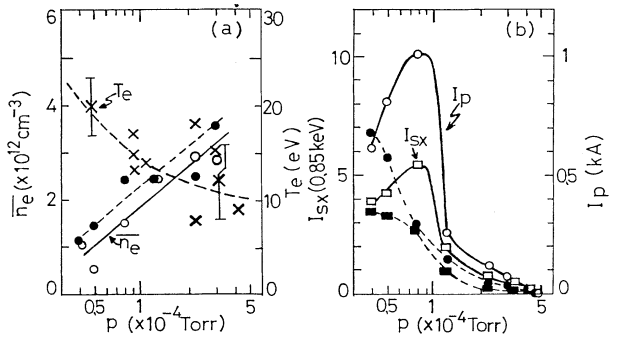

FIG. 3. (a) Electron density $\bar{n}_e$ and temperature T_e as functions of p. (b) Plasma current I_p (open circles, filled circles) and soft x-ray I_{sx} (open squares, filled squares) as functions p. Solid curves are for LH-CS plasmas produced in ECR plasma; dashed ones for ECR plasma alone. $P_{ECH} = 20$ kW, $P_{LHH} = 20$ kW, and $B_v = 11$ G (steady).

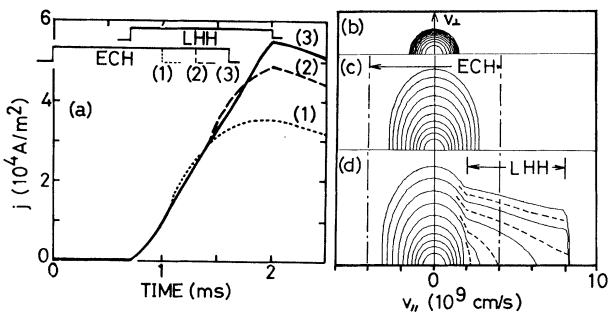

FIG. 4. (a) Temporal evolution of plasma current density J_p for various pulse lengths of P_{ECH}. (b)–(d) Contours of constant velocity distribution function in $v_\parallel$, $v_\perp$ phase space at (b) $t = 0$, (c) 0.6 ms (P_{ECH} being injected), and (d) 1.2 ms (P_{ECH} and P_{LHH}).

distribution of electrons. For the actual ECR plasma, a weak current I_p is flowing and its direction is such that B_v makes better confinement for the current-carrying electrons against the toroidal drift.[12]

In conclusion, the toroidal plasma current I_p can be started up and sustained by injecting P_{LHH} into the ECR plasma without the Ohmic heating power (rf tokamak). Sustainment of I_p suggests the steady operation of the tokamak reactor. Startup of the tokamak discharge by rf alone is very useful, since the device becomes simple without the Ohmic heating transformer or its volt-seconds can be saved. It is noted that half of the total volt-seconds are dissipated during the startup even in the INTOR.[13] Physically it is shown that the high-energy tail electrons in the initial ECR plasma are necessary to generate LHW-driven current. The result suggests that such a current can be generated in high-density plasmas above the density limit if the high-energy electrons are produced by ECH.

[1]N. J. Fisch, Phys. Rev. Lett. 41, 873 (1978).
[2]J. D. Cordey *et al.*, Plasma Phys. 24, 73 (1982).
[3]S. Y. Yuen *et al.*, Nucl. Fusion 20, 159 (1980).
[4]T. Yamamoto *et al.*, Phys. Rev. Lett. 45, 716 (1980).
[5]T. Maekawa *et al.*, Phys. Lett. 85A, 339 (1981), and Nucl. Fusion 23, 242 (1983); M. Nakamura *et al.*, J. Phys. Soc. Jpn. 51, 3696 (1982).
[6]S. C. Luckhardt *et al.*, Phys. Rev. Lett. 48, 152 (1982).
[7]K. Ohkubo *et al.*, Nucl. Fusion 22, 203 (1982).
[8]M. Nakamura *et al.*, Phys. Rev. Lett. 47, 1902 (1981); S. Tanaka *et al.*, in Proceedings of the Ninth International Conference on Plasma Physics and Controlled Nuclear Fusion Research, Baltimore, Maryland, September 1982 (to be published), paper No. IAEA-CN-41/C-1-3.
[9]S. Bernabei *et al.*, Phys. Rev. Lett. 49, 1255 (1982).
[10]M. Porkolab *et al.*, in Proceedings of the Ninth International Conference on Plasma Physics and Controlled Nuclear Fusion Research, Baltimore, Maryland, September 1982 (to be published), paper No. IAEA-CN-41/C-4.
[11]L. A. Artsimovich, Nucl. Fusion 12, 215 (1972).
[12]M. Nakamura *et al.*, Phys. Lett. 81A, 383 (1981).
[13]INTOR Group, *INTOR Phase One* (IAEA, Vienna, 1982), Chap. 3.